Energy 198 (2020) 117301

Contents lists available at ScienceDirect

Energy

journal homepage: www.elsevier.com/locate/energy

Exploring high-penetration electric vehicles impact on urban power grid based on voltage stability analysis

Lin Lyu [a], Xinran Yang [a, b], Yue Xiang [a, *], Junyong Liu [a], Shafqat Jawad [a], Runqi Deng [a]

[a] College of Electrical Engineering, Sichuan University, Chengdu, 610065, China
[b] Guangzhou Power Supply Bureau, Guangdong Power Grid Co., Ltd., Guangzhou, 510620, China

ARTICLE INFO

Article history:
Received 25 July 2019
Received in revised form
23 January 2020
Accepted 1 March 2020
Available online 3 March 2020

Keywords:
Electric vehicles
Voltage stability
Coupled transportation and distribution networks
Mobile energy
The worst charging case

ABSTRACT

Electric vehicles (EVs) have received significant attention in recent years. The high penetration of EVs increased the charging load in the distribution network, which has an enormous impact on "transportation and power grid" coupled energy networks. This paper developed the models and methods to evaluate the capacity of electrical energy supply based on voltage stability in the worst charging case scenario, under the existing coupled network. An optimization method with transportation network constraints is proposed to find the worst charging case scenario. In addition, the mobility of EVs is considered to calculate the load margin and the maximum number of EVs charging that a given grid can support in the critical situation. The method and model are simulated by test cases, which provide a perspective for realizing the EVs integration capacity limitation in urban areas considering the coupling relationship between transportation and power grids. Finally, the impact of charging location and route choice in the voltage margin limitation is emphasized.

1. Introduction

It is widely accepted that electric vehicles (EVs) are an effective solution to reduce greenhouse gas emissions, especially CO_2, and change the structure of energies in urban area [1]. The level of emissions may be significantly affected by the management of EVs, and EVs is one of the most effective ways of solving environmental problems [2]. Also, the coordination of EVs and distributed generations may further reduce greenhouse gas further [3,4]. As a result, more and more countries have considered the popularization of EVs as one of the most prominent national plans [5,6]. On the other hand, the rapid development of EVs also brings various challenges to the power grid for increasing charging demand [7]. Therefore, it is necessary to evaluate the impact of EVs on the power grid under the worst charging case.

The impact of charging load on the power grid can be delimited in two significant aspects, including the variation of charging location and the random of charging time caused by the decision behavior during driving. There is extensive research in this field, for instance, the voltage stability at a given moment based on a given charging load at the bus of the power grid, which is determined by the driving behavior is evaluated in [8]. Based on the large scale investigation of charging demand, the influence of different penetration charging load on voltage stability is introduced in reference [9]. The impact of charging load on voltage and the peak-valley difference of load analyzed in [10], where a certain percentage of charging load integrated into some designated bus of the power grid. These studies can be considered as static studying, i.e., the value and position of charging load is given before evaluation. Their drawbacks are regardless of the spatial and temporal variation of charging load due to the transfer properties of mobile energy caused by the mobility of EVs in the vehicle energy network.

Besides, most of the charging load models are proposed based on the characteristic of daily trips with probability distribution function. The aggregation model of charging station is proposed based on the charging load curve in reference [11], and the behavior of EVs is described by second-order Position distribution. Reference [12] presented a charging demand model based on the EV probability distribution of each region in a different time, and the variation of mobile energy is described by Markov chain. The literature above only investigated the driving characteristic without constraints of a transportation network to EVs route and charging behavior, which have an impact on charging load distribution.

In addition, existing research mainly focuses on coordinated

* Corresponding author.
E-mail address: xiang@scu.edu.cn (Y. Xiang).

https://doi.org/10.1016/j.energy.2020.117301
0360-5442/

charging strategy and optimization of charging. Based on the proposed demand-side management, EV owners were guided for charging at an appropriate location to make full use of the power from distributed generations [13]. A multi-stage optimal scheduling approach considering charging load was proposed to smooth the fluctuation caused by renewable resources and EVs [14]. An integrated tool [15] was proposed to manage voltage deviation through coordinating the controllable loads such as EVs. Considering the realistic setting, EV coordinated charging strategy was formulated as two successive binary model in [16]. Ref. [17] conducted an optimal strategy with integration of EVs to maximize benefit. It was investigated in [18] that coordinated charging strategy is beneficial for frequency deviation in the presence of EVs participating in microgrid. An optimal charging-discharging model was introduced in [19] to realize economic operation, where EV behavior was described by a statistic model. Nowadays, there are some new approach applied in this field, such as cyber-physical system (CPS) approach since the integration of EVs and power grid is a typical example of cyber-physical system. Ref. [20] proposed a CPS-based collaborative design optimization approach which is suitable for automatic control of EVs. A CPS-based control framework is presented to optimize the fuel consumption and safety for vehicle systems in [21]. However, the proposed work mainly focused on the impact of EVs on the power grid in the worst charging case to find the worst charging location and driving path under the existing coupling relationship between transportation network and distribution network. Although some researchers have been investigated the negative impact of charging load on the power grid, however, their main purpose is to investigate the coordinated charging strategy, rather than evaluating the adverse effect of charging load on the power grid. For example, the load curve between coordinated charging and general charging was compared in [22]. The result shows the spatial and temporal advantages of adjusting the EV charging load with the low load period by coordinated charging strategies. Ref. [23] proposed an effective contribution of coordinated charging strategies to reduce the charging costs and peak load by comparison between optimal charging strategy, suboptimal strategy and uncoordinated charging scenarios. More importantly, individual analysis on the negative impact of disordered charging on the power grid was not considered. And there are many researches about voltage stability in distribution network, such as references [24–26]. A novel method is proposed to predicted voltage collapse using the critical transition theory in [24]. Newton-Raphson technique is used to solve a line-wise set of equations modelling a power system to analyze voltage collapse in [25]. Ref. [26] proposed a new normalized voltage stability indicator called P-index to indicate the margin of voltage collapse. However, the novelty of this article is that providing a method to evaluate the impacts of large scale of EVs on distribution network in worse charging case considering the EVs mobility from the perspective of voltage stability, rather than a novel method to evaluate voltage stability.

In the view of the integration of EVs in transportation and power grid, not only charging demand should be considered, but also EVs have features on traffic vehicles, which leads to their behavior and mobile energy are affected by the transportation network structure and traffic flow that is called vehicle energy network. Some literature focused on the coupled network between transportation and power grid. The mobility of EV was considered in [27], where EV charging demands was predicted with origin-destination pairs in coupled transportation and power network. Ref. [28] focused on the EV charging in the coupled network considering variation in electricity prices caused by congestion in the power grid. Ref. [29] studied a reliability evaluation method for a coupled network of the transportation network and power grid with EVs.

Consequently, this paper aims to propose a method to evaluate the impacts of large scale of EVs on distribution network in worse charging case from the perspective of voltage stability considering the coupled traffic-electric network. In particular, an optimal model is used to identify the worst charging case with minimum voltage margin, which examines the constraints of the transportation network to charging location and driving path. The assessment method is based on voltage stability analysis, which determines the critical point of voltage by continuous power flow. In order to achieve an effective reflection on the mobility of EVs, vehicles energy caused by the mobility of EVs in the transportation network are introduced in this paper, also an improved continuous power flow with EVs is proposed to calculate the load margin. The novelty of this paper is to take deep insights of the mobile energy, vehicle energy network, and electricity energy network when modelling charging load in the distribution network, and evaluate the negative impact of mobile energy on electricity energy network in the worst charging case based on voltage stability analysis. The organization of the integrated energy network is depicted in Fig. 1. The mobile energy of EVs links the vehicle energy network and electricity energy network, owing to consumption in the transportation network and charging in the power grid.

The rest structure of this paper is presented in Fig. 2. In section 2, the coupled network modelling of vehicle energy network and electricity energy network is presented. Then, in section 3, the worst charging case is proposed by design the route of EVs based on mobile energy consumption, and obtained by an optimal model. In section 4, an improved continuous power flow with EVs is proposed to identify the critical point of the electrical energy network and evaluate the voltage stability. The test case is shown in section 5. And finally, section 6 summarizes the proposed study.

2. Coupled network modelling

Considering a strong connection between transportation network and distribution network, the coupled network of them is presented by a complicated matrix $\boldsymbol{A}$ as Equation (1), where $\boldsymbol{A}_{\mathrm{T}}$ is the matrix of the transportation network that will be discussed in detail in 2.2.1, $\boldsymbol{A}_{\mathrm{P}}$ is the admittance matrix of distribution network and $\boldsymbol{A}_{\text{T-P}}$ is the coupling matrix of them. $a_{\mathrm{T},ab}$ of $\boldsymbol{A}_{\mathrm{T}}$ depicts the information of transportation network node between a and b. Similarly, $a_{\text{T-P},aj}$ of $\boldsymbol{A}_{\text{T-P}}$ is the information between the transportation network node a and distribution network bus j. If they are coupled, $a_{\text{T-P},aj} = 1$, otherwise $a_{\text{T-P},aj} = 0$.

$$\boldsymbol{A} = \begin{bmatrix} \boldsymbol{A}_{\mathrm{T}} & \boldsymbol{A}_{\mathrm{T-P}} \\ \boldsymbol{A}_{\mathrm{T-P}}^{\mathrm{T}} & \boldsymbol{A}_{\mathrm{P}} \end{bmatrix} \tag{1}$$

In geographic location, the charging station around transportation network node is connected to the nearest substation by electrical cables. Though each pair of transportation network node and distribution network bus is not the same geographically, they are coupled by the complicated matrix $\boldsymbol{A}$ with mobile energy of EVs as shown in Fig. 3.

2.1. EVs charging model

Each EV information comprises geographical location and the state of charge (SOC) at any time. From reality, we assume that the state of EV includes driving, parking and charging, which is presented by Equation (2). Noted that we don't consider the discharging, because the motivation of this paper is that propose a method to evaluate the impact of EVs on power grid in worse charging case considering more and more EVs are introduced to urban cities, and they also bring challenges to power grid. Besides,

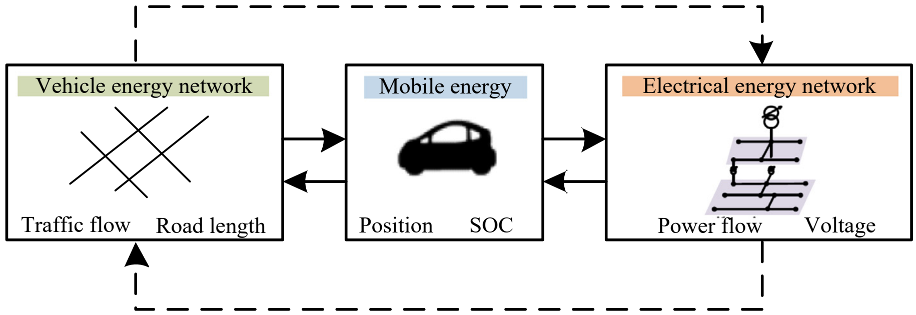

Fig. 1. Integrated networks.

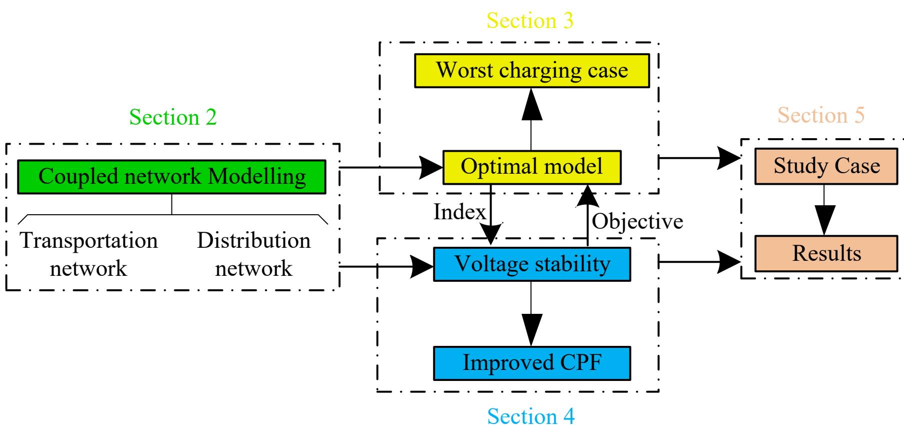

Fig. 2. Integrated framework.

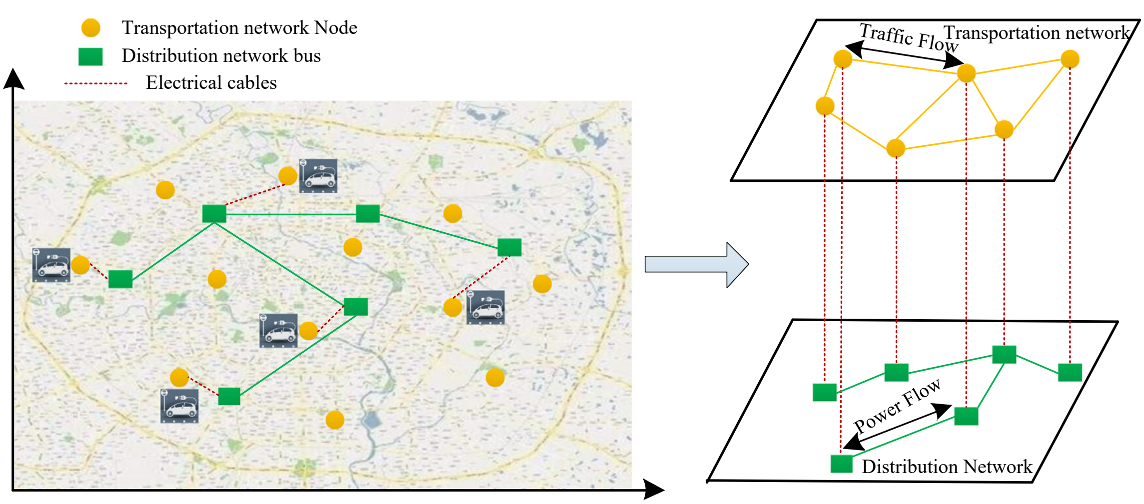

Fig. 3. Coupled networks.

the state of EV is determined by vehicle energy information and electrical energy distribution, which is the same the other way round. The state of EV has an effect on vehicle energy and electrical energy distribution in a coupled network.

$$s_t = \{-1, 0, 1\} \tag{2}$$

where, s_t is the state of EV at time t. $s_t = -1$ represents EV is driving, if EV is parking, $s_t = 0$, and $s_t = 1$ represents the EV is charging.

Several charging methods have been proposed in the literature, such as charging once a day [30], charging at a given time [31], a coordinated charging strategy based on demand response [32], and so on. To underline the disordering of charging, the taxi is chosen to study with fast charging. SOC is calculated by Equation (3), for simplifying, we assume the charging power is constant, and the power consumption is only related to mileage.

$$SOC_{t+1} = \begin{cases} SOC_t + \dfrac{P_c T_c}{Q} & s_t = 1 \\ SOC_t & s_t = 0 \\ SOC_t - \dfrac{\omega l}{Q} & s_t = -1 \end{cases} \tag{3}$$

where, SOC_t is the SOC at time t. P_c represents the charging power, T_c represents the charging time, and Q is the battery capacity. When $s_t = -1$, ω is the power consumption per mile and l is mileage during the last trip.

2.2. Transportation network model

1) Formulation of Transportation Network

The traffic is composed of node and road, for simplifying, which is represented by $\boldsymbol{A}_{\mathrm{T}}$ ($\boldsymbol{V}$, $\boldsymbol{D}$) in brief, where $\boldsymbol{V} = \{v_{\mathrm{T},a} | a = 1,2, \ldots, n\}$is the set of nodes and $\boldsymbol{D} = \{d_{ab} | a,b = 1,2, \ldots, n\}$is the set of road length. Here, the n is the number of transportation nodes, a and b is the transportation node. The formulation of Fig. 4 is shown in Equation (4). Noted that the difference of the each road is shown by parameters C_{ab}, β_{ab}, μ, γ, q in Equation (5).

$$\boldsymbol{A}_{\mathrm{T}} = \begin{bmatrix} 0 & d_{12} & d_{13} & \inf & d_{15} \\ d_{12} & 0 & \inf & d_{24} & \inf \\ d_{13} & \inf & 0 & d_{34} & d_{35} \\ \inf & d_{24} & d_{34} & 0 & \inf \\ d_{15} & \inf & d_{35} & \inf & 0 \end{bmatrix} \tag{4}$$

where, the value of $a_{\mathrm{T},ab}$ is the road length between node a and b. Noted that $a_{\mathrm{T},ab} = \inf$ if they are nonadjacent.

The speed of EV is associated with the capacity of road and traffic flow when choosing the driving route [33], can be formulated as Equation (5) [34].

$$\begin{cases} v_{ab}(t) = \dfrac{v_{ab,0}}{1 + \left(\dfrac{V_{ab}(t)}{C_{ab}}\right)^{\beta_{ab}}} \\ \beta_{ab} = \mu + \gamma \left(\dfrac{V_{ab}(t)}{C_{ab}}\right)^{q} \end{cases} \tag{5}$$

where, $v_{ab,0}$ is the maximum accepted speed of road ab, $V_{ab}(t)$ is the traffic flow of road ab at time t. The C_{ab} presents the road capacity of road ab. β_{ab} is the saturation coefficient of road ab at time t. Other variables like μ, γ, q are adaptive parameters that can be given by the measured data.

2) Method for Routing Path Selection

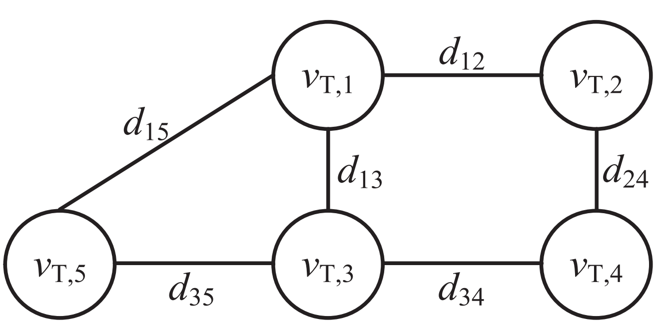

Fig. 4. Topological structure of transportation network.

There are multiple traffic paths between node a and b. Besides, routing path selection varies from different perspectives, such as the shortest time-consuming, the shortest path, and so on. In this paper, the shortest path is selected as the routing path. The set of all feasible path between a and b is $\boldsymbol{L}_{ab}$ that is obtained with the Warshall method [35] based on $\boldsymbol{A}_{\mathrm{T}}$. The shortest path $l_{ab} = \{a, \ldots, u, v, \ldots b\}$ is determined by the Floyd algorithm [36], which is shown as Equation (6). Here, u and v are the nodes between a and b.

$$\mathrm{Min}\left(\sum_{u,v \in \boldsymbol{L}_{ab}(s)} a_{\mathrm{T},uv}\right) \tag{6}$$

3. The worst charging case

Different driving routes produce different SOC variation and charging demand. Thus the energy of EV is related to mobile qualities. In order to explore the impacts of the variation of mobile energy on the power grid, the worst charging case is designed by planning the EVs route considering the constraints of the transportation network to EVs, where voltage is close to the limit. Because voltage is one of the important indexes to evaluate the stability of the power system [13,37].

The worst charging case model can be described in details as following. This model is multi-restrained nonlinear equations, which is solved by Particle Swarm Optimization. The solution of this model means the charging load is obtained, including the value and location, then the voltage stability can be analyzed.

1) Objective function: The goal of this model is to find the worst charging case, thus makes the distribution network runs much close to the limit, as shown in Equations (7)–(10, where considering the constraints for state variables (Equation (9)). Here, F is the objective function, F_{u} is the deviation of actual voltage from the optimal value with the maximum margin, λ is the penalty coefficient, which constraints for state variables, including transmission power of lines and voltage of nodes, as shown in Equation (9). The value of penalty coefficient is set comparatively large to ensure the transmission power and voltage within the available range. $\boldsymbol{Y}$ is the matrix of the optimal voltage of all buses calculated by optimal power flow, where the objective is the least power losses with the same total load, $\boldsymbol{H}(\boldsymbol{X})$ is the matrix of the actual voltage of all buses. C_e and u_f are transmission power of line e and voltage of bus f respectively, $C_e^{\max}$ and $C_e^{\min}$ are the upper and lower limits for the transmission line e, $u_f^{\max}$ and $u_f^{\min}$ are the upper and lower limits for the bus f, N_{L} is the set of transmission lines, M is the number of buses, $\varepsilon(R)$ is a function with 0 or 1, where R can be any real number.

$$F = \max\{F_{\mathrm{u}} - \lambda F_{\mathrm{s}}\} \tag{7}$$

$$F_{\mathrm{u}} = [\boldsymbol{Y} - \boldsymbol{H}(\boldsymbol{X})][\boldsymbol{Y} - \boldsymbol{H}(\boldsymbol{X})]^{\mathrm{T}} \tag{8}$$

$$F_{\mathrm{s}} = \sum_{e}^{N_{\mathrm{L}}} \varepsilon\left(C_e - C_e^{\max}\right) + \sum_{e}^{N_{\mathrm{L}}} \varepsilon\left(C_e^{\min} - C_e\right) + \sum_{f}^{M} \varepsilon\left(u_f - u_f^{\max}\right) + \sum_{f}^{M} \varepsilon\left(u_f^{\min} - u_f\right) \tag{9}$$

$$\varepsilon(R) = \begin{cases} 0 & R < 0 \\ 1 & R \geq 0 \end{cases} \forall R \tag{10}$$

2) Decision variables: The decision variables are available EVs and corresponding charging load, which can be derived from Equations (11)-(12). Where, p is the EV that satisfies the charging condition, N_V is the number of EVs, and the s^p is the state of EV p, P_{EV} is the charging load.

$$p \in [1, N_V] \tag{11}$$

$$P_{EV} = P_c \sum_{p}^{N_V} s^p \tag{12}$$

3) Constraints: The equality constraints are the power balance equations that include the grid losses, which are given as Equation (13), where, $\boldsymbol{G}_P$ and $\boldsymbol{G}_Q$ are the vectors of active and reactive power. $\boldsymbol{P}_0$ and $\boldsymbol{Q}_0$ are the active and reactive power of electricity load respectively.

$$\begin{bmatrix} \boldsymbol{G}_P \\ \boldsymbol{G}_Q \end{bmatrix} = \boldsymbol{A}_P \begin{bmatrix} \boldsymbol{P}_0 + \boldsymbol{P}_{EV} \\ \boldsymbol{Q}_0 \end{bmatrix} \tag{13}$$

The inequality constraints comprise three rules. The first rule is the difference in mobile energy between origin and destination nodes are higher than the power consumption in this distance. Also, we assumed the upper and lower value of battery level to prolong the service time of the battery and set up charging condition, as shown in Equation (14). The second rule is the SOC and charging time (Equation (15)-(16)), which are restrictions for charging until SOC^{max} or next evaluation. The last rule is that the total driving time spends on the distance between origin and destination has to be smaller than the deviation between the following time considering the constraint of the transportation network, as stated in Equation (17). Here, $\underline{\alpha}$ is the minimum threshold coefficient of battery, α is the threshold coefficient of charging condition, T_t is the evaluation moment at time t

$$\underline{\alpha}Q \leq SOC_t^p Q - s_t^p \omega l_{t+1}^p \leq \overline{\alpha}Q \tag{14}$$

$$\overline{\alpha}Q \leq SOC_t^p Q + P_c s_t^p T_{t,c}^p \leq SOC^{max} Q \tag{15}$$

$$T_t - T_{t-1} - l_t^p \Big/ v_t^p \leq T_{t,c}^p \leq T_{t+1} - T_t \tag{16}$$

$$l_t^p \,/\, v_t^p \leq T_{t+1} - T_t \tag{17}$$

4. Voltage stability in the worst charging case

4.1. Improved continue power flow with EVs

The electricity energy network stability is evaluated based on voltage stability. Continuous Power Flow (CPF) is the primary method to search for the critical point of voltage [38,39], however, charging load is different from electricity load, due to charging load variation in spatial and temporal caused by EVs mobility. Therefore, it is necessary to propose an improved CPF (Equation (18)-(19)) to calculate the maximum load in the distribution network.

$$\begin{aligned} P_{L,i} &= \zeta_i K_P P_{L,i0} \\ Q_{L,i} &= \zeta_i K_Q Q_{L,i0} \end{aligned} \tag{18}$$

$$F(\boldsymbol{\theta}, \boldsymbol{V}, \boldsymbol{\zeta}) = 0 \tag{19}$$

where, $P_{L,i}$ and $Q_{L,i}$ are the active power and reactive power at bus i, $P_{L,i0}$ and $Q_{L,i0}$ are the original active power and reactive power at bus i. ζ_i is the load parameter of bus i, which is related to the number of EVs integrated with this bus, and the value is an integer multiple of the P_c. Hence, $\boldsymbol{\zeta}$ is a multi-dimensional variable as the time goes and is changed with EVs number increase. K_P and K_Q is the load multiplier at bus i that stands for proportional coefficient of active and reactive power growth. The voltage amplitudes and the voltage phases are represented by vector $\boldsymbol{V}$ and $\boldsymbol{\theta}$.

4.2. Electricity load generation

Electricity load is defined as all of the load in the distribution network, except for charging load. Electricity load is still volatile, therefore the value of the electricity load is obtained by Latin Hypercube Sampling (LHS) [40]. The procedure of sampling is detailed below.

Let's assumed that the set of electricity load is $\boldsymbol{L}_{el} = [L_1, L_2, \ldots, L_M]$,where, the M is the number of buses, and the original load of bus k is L_{k0}. The maximum load of bus k is L_{k1} obtained by the approach of only increasing the load in this bus to the limits, thus the maximum growth factor is $\delta_{k,max} = L_{k1}/L_{k0}$. The growth factor δ_k can be described by a uniform distribution at $[\theta_k/L_{k0}, \delta_{k,max}]$, here, θ_k is the lower limit of bus k.

The cumulative distribution function (CDF) of δ_k can be expressed as Equation (20).

$$Y_k = Z_k(\delta_k) \tag{20}$$

where, Y_k is an increasing function from 0 to 1. $[\theta_k/L_{k0}, \delta_{k,max}]$ is divided into N segments. Y_{ki} is sampled at each segment. The sampling matrix $\boldsymbol{X}_k$ is obtained by the inverse function of Equation (20), then put them in order according to the Gram-Schmidt method [41]. Thus the sampling matrix of growth factor of electricity load is given as $\boldsymbol{\delta}$.

4.3. Voltage assessment procedure

The assessment procedure is as follows: first, according to the trend of deteriorating voltage stability, obtain the possible charging load location. Second, choose the route path to charging location in geography. Then, checking the constraints of SOC and time based on selection route path. Last, evaluate the voltage stability or come back. The procedure flowchart is shown in Fig. 5.

The steps of voltage stability evaluation is summarized as follows.

1) Set the initial position of each EV, initial travel moment, and initial SOC, namely D_0, $T_{start,}$ and SOC_0.
2) Increase load at each bus to the limited state based on equal probability. $L_{k\_collapse}$ is the critical load at bus k, and the growth factor $\delta_{collapse} = L_{k\_collapse}/L_{k0}$ is the criterion of the voltage limit of this bus.
3) Obtain the matrix of integrated load growth factor $\boldsymbol{S}_{M \times N}$ according to the electricity load generation and the demand for charging load. Noted that each column of $\boldsymbol{S}_{M \times N}$ stands for a load state. If max $(S_{kj}) < \delta_{collapse}$, eliminates this column due to this state is far away from the critical point. Similarly, eliminates this

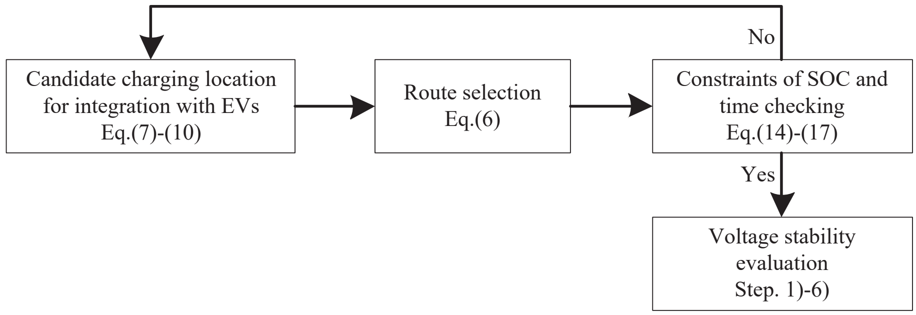

Fig. 5. Procedure flowchart.

column, if min $(S_{kj}) > \delta_{\text{collapse}}$, because this state is out of stability. Thus $\boldsymbol{S}_{\text{M}\times\text{N}}$* is obtained.

4) To choose the point near to the critical state further, every two columns are compared. If min $(s_{kr}) >$ max (s_{kt}), eliminates the column t. $\boldsymbol{S}_{\text{all}}$ is got from $\boldsymbol{S}_{\text{M}\times\text{N}}$*, where each point is close to critical state.
5) Calculate the growth factor matrix $\boldsymbol{S}_{\text{all}}$* for every state chosen from each column of $\boldsymbol{S}_{\text{all}}$ by the improved CPF proposed in 4.1.
6) Repeat the steps from 3 to 6. The N_{sample}/N obtains the repetition, here, N_{sample} is the sampling times we assumed.

5. Case studies

5.1. Case description

A part of an urban transportation network [42] is used as the test case, which contains 29 nodes and 47 roads that average length is 2.92 km, also this transportation network is divided into three areas, residential, commercial and industrial, as shown in Fig. 6.

12.66 kV 33-bus distribution network [43] is used as the corresponding distribution network, which is shown in Fig. 7. The detailed line parameters can be found in Table 1. The corresponding coupled relationship between the transportation network and distribution network is listed in Table 2.

It is assumed that the initial location of EVs are transportation node 2, 3, 4, 8 and 12 randomly, also $\text{SOC}_0 = \text{SOC}^{\max}$. According to reference [44], the parameters of PHEV60 are used to simulate the charging feature of EVs. The charging power is 9 kW, if the EVs charges at the charging station, and the energy consumption is 0.24 kWh/mile, also, $\underline{\alpha}$ is set as 0.1, and α is set as 0.6.

5.2. Case results and analysis

The worst charging case for the coupled network is used in test cases. Fig. 8 depicts the voltage distribution at critical points.

As seen in this figure, the voltage of each bus varies with time. However, the weakest bus area value lower than normal bus is consistent, such as buses 10, 11, 14 and 15. The perspective of the vehicle energy network, these buses are connected to transportation node 8, 9, 14, and 15, as shown in Fig. 9.

Besides, these transportation nodes have a lot in common. They are mostly located between residential and commercial areas. The reason for this feature is that these two areas have sufficient electricity load. Charging load will add a heavy burden to the distribution network, namely, more demand for electricity energy appears. In particular, if the voltage of these areas collapses, the electrical energy supply will be interrupted, causing severe loss in society and power system. Therefore, the bus integrated with charging station should be changed or the capacity of these substations should be expanded to ensure the stability of supplying electrical energy, when reform the distribution network or charging network.

Also, Fig. 10 shows the load margin for one of the weakest bus 15 in different charging cases. There is a significant difference in

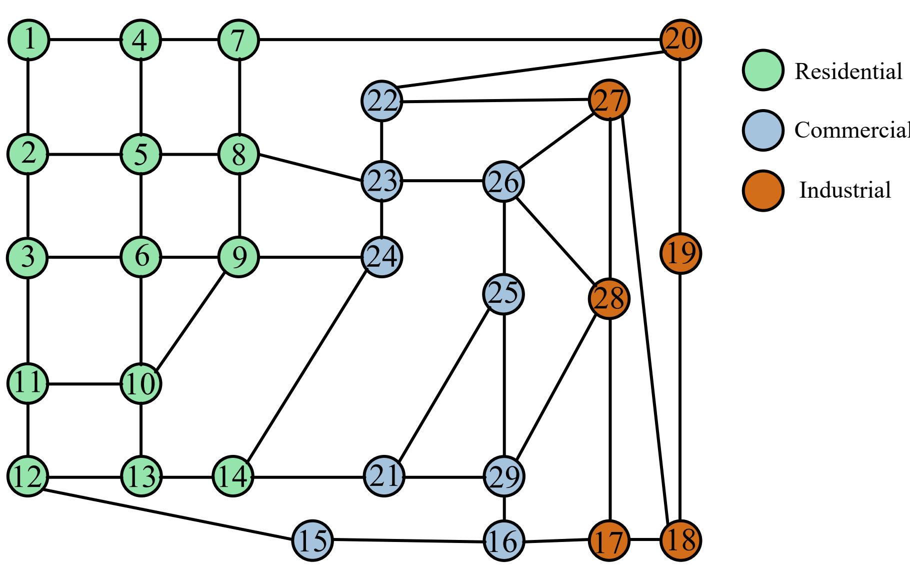

Fig. 6. Urban transportation network.

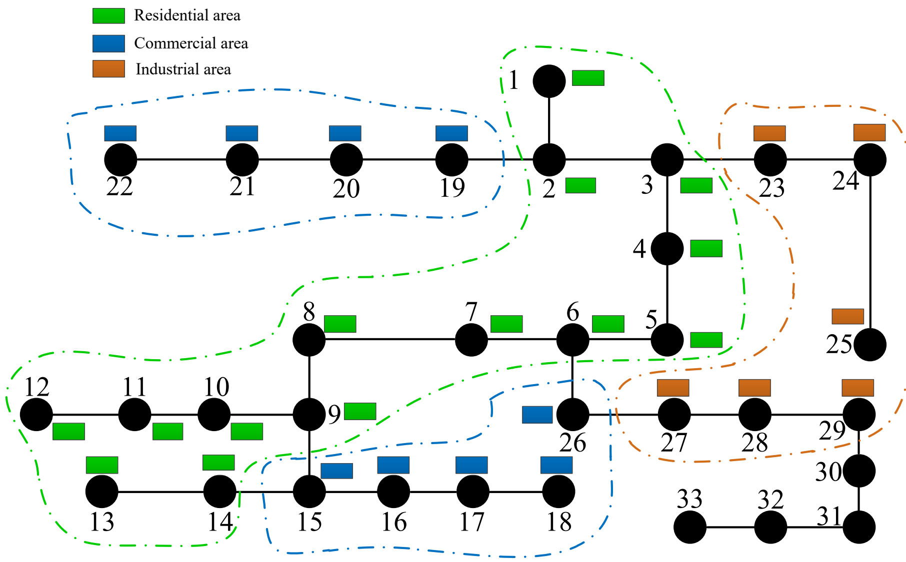

Fig. 7. 33-bus distribution network.

Table 1
Line parameters of the 33-bus distribution network.

Line #	Starting bus	Ending bus	Resistance	Reactance	Line #	Starting bus	Ending bus	Resistance	Reactance
1	1	2	0.0922	0.047	17	10	11	0.1966	0.065
2	21	22	0.7089	0.9373	18	9	10	1.044	0.74
3	20	21	0.4095	0.4784	19	9	15	2	2
4	19	20	1.5042	1.3554	20	13	14	0.5416	0.7129
5	2	19	0.164	0.1565	21	14	15	0.591	0.526
6	2	3	0.493	0.2511	22	15	16	0.7463	0.545
7	3	23	0.4512	0.3083	23	16	17	1.289	1.721
8	23	24	0.898	0.7091	24	17	18	0.732	0.574
9	7	8	0.7114	0.2351	25	32	33	0.341	0.5302
10	6	7	0.1872	0.6188	26	31	32	0.3105	0.3619
11	5	6	0.819	0.707	27	26	27	0.2842	0.1447
12	3	4	0.366	0.1864	28	27	28	1.059	0.9337
13	4	5	0.3811	0.1941	29	28	29	0.8042	0.7006
14	8	9	1.03	0.74	30	28	30	0.9744	0.963
15	6	26	0.203	0.1034	31	29	30	0.5075	0.2585
16	11	12	0.3744	0.1238	32	24	25	0.896	0.7011

Table 2
Corresponding node numbers between distribution network and transportation network.

Distribution bus	Transportation node	Distribution bus	Transportation node	Distribution bus	Transportation node
1	1	12	12	23	25
2	2	13	13	24	27
3	3	14	14	25	28
4	11	15	15	26	29
5	4	16	16	27	17
6	5	17	23	28	18
7	6	18	24	29	19
8	10	19	26	30	–
9	7	20	20	31	–
10	8	21	21	32	–
11	9	22	22	33	–

multiples of load growth with varying behaviors of charging. In the worst charging case, the load margin of this bus is smaller than another. It means the distribution network produces different electricity energy margin in different charging cases and the availability of supplying electrical energy of distribution network will not meet the electrical energy demand in extreme situation if a large amount of EVs integrated into distribution network or electricity load increasing. The result indicates that the collapse of the electrical energy network is more direct than expected, which deserved serious consideration while evaluating the security of the distribution network. And Fig. 11 is the P–V curves of bus 14 in different scenarios. It should be noted that k^L represents the multiples of electricity load.

To understand the importance of coupling relationship between the transportation network and distribution network to the capacity of electrical energy supply, the result of two testing cases are

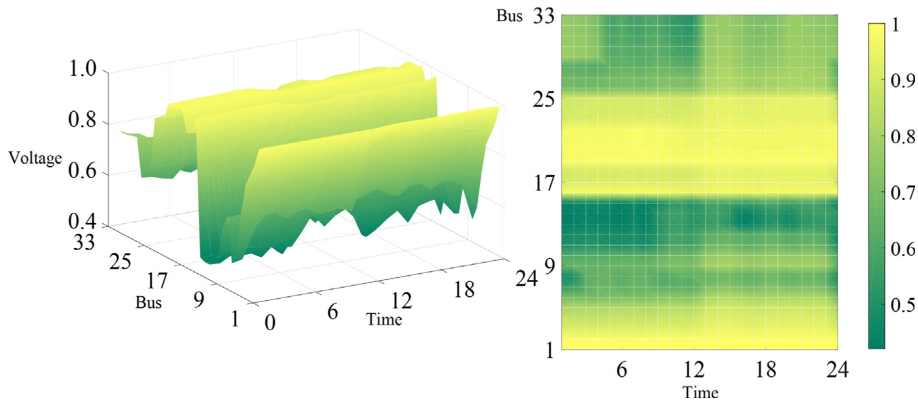

Fig. 8. Voltage distribution.

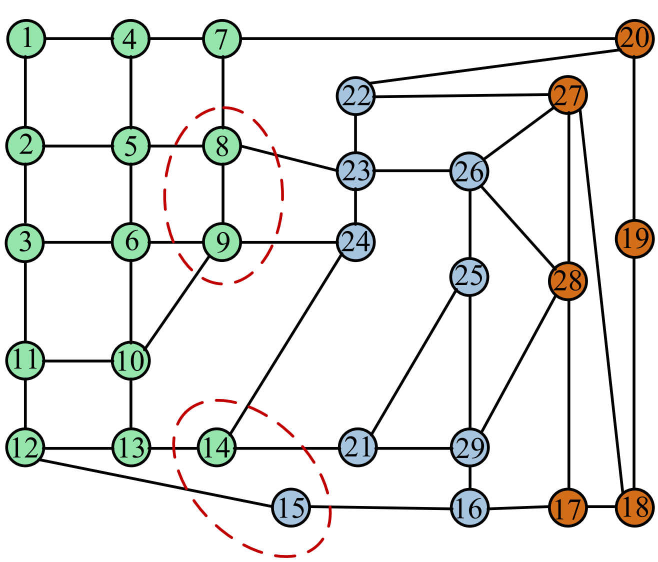

Fig. 9. Weakest area in transportation network.

illustrated in Table 3. The corresponding node numbers of coupled energy network of case a) as shown in Table 2, in the case b), coupling relationship between node 15 and bus 33 replace node 15 and bus 33.

A significant t difference is observed of growing load multiples with different coupling relationship, which indicates the electricity energy network stability in case b) is stronger than case a). The reason for such difference is that mobile energy demand is far from heavy electricity load buses, such as bus 15, which relieves the electricity energy burden in the local region. Thus, for the same electrical energy demand, changing the coupling relationship between the transportation network and distribution network is an effective method to obtain more electricity energy margin in the distribution network and avoid electricity energy interruption. According to the results, the voltage stability is influenced by the coupling relationship between transportation network and distribution network, which indicates the coupled network reformation.

The different routes of EVs consume different mobile energy, thereby causing different charging load on the corresponding electrical energy network. To ensure the distribution network operates in an emergency, the destination node in transportation network is given, if the coupled relationship between transportation network and distribution network is specified, which indicates that the corresponding route of EVs could be generated, as shown in Table 4.

EVs at different original node have different destination node based on the worst charging case, as shown in Fig. 11. For the destination node 5, EV #1 is closer to node 11 than EV #5, however, in actual, this destination node is allocated to EV #5, because the proposed strategy considers the energy consumption during driving that associated with path length. The distance between the origin of EV #1 and destination node 5 is the only 1.8 km, mobile energy consumption in this way is too small to satisfy the charging

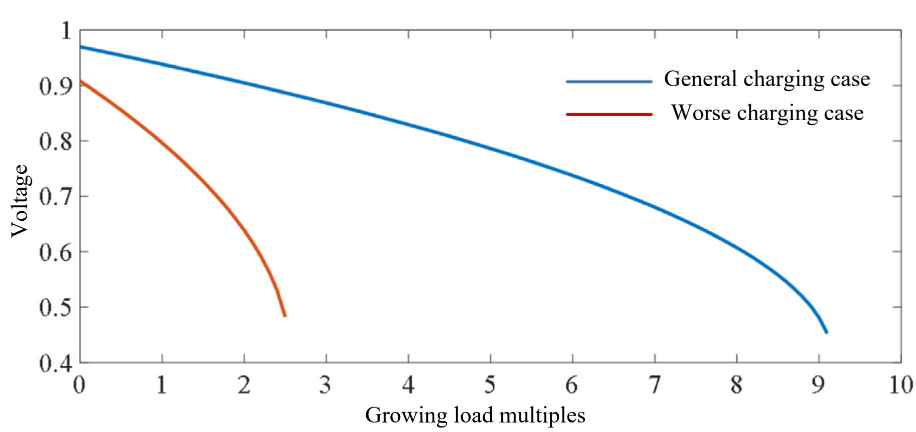

Fig. 10. Load Margin of bus 15 in different scenarios.

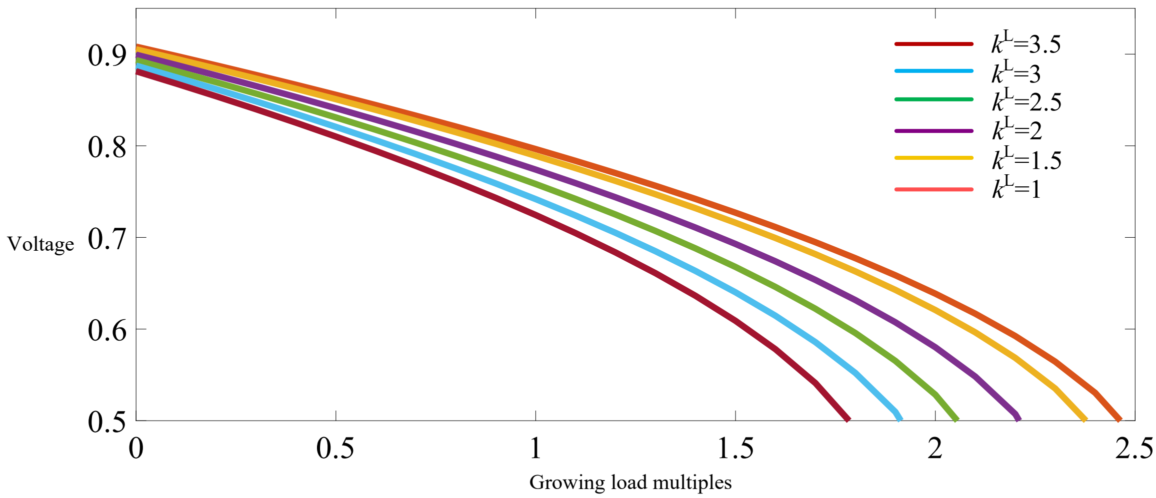

Fig. 11. Load Margin of bus 14 in different scenarios.

Table 3
Corresponding growing load multiples in cases.

Case	a)	b)
Growing load multiples	2.3	4.0

Table 4
Route path between origin and destination.

EV #	Route
1	2-5-8-9-10-11
2	3-6-5-8-23-26; 3-11-12-15
3	4-7-20-19-18; 4-5-6-3-2-1
4	8-7-20-22; 8-9-10-11-3
5	12-13-10-6-5

condition, based on Equation (14), thus, it can be ignored. Importantly, the charging load depends on the routing choice, which indicates how to guide the EVs behavior to guarantee the voltage stability.

Regarding the impact of routes that have the same origin and destination on mobile energy, two different routes are designed, as follows:

1) Route 1: 2-5-8-9-10-11;
2) Route 2: 2-3-11.

Different routes generate different SOC is shown in Fig. 12, where the red dashed line represents the threshold battery for charging as α in Equation (14). The result indicates that the transportation network is an important factor affecting the EVs mobile energy and charging behavior, which leads to the variation of charging demand in the electrical energy network.

However, the above reason doesn't fit for all of the destination allocations. The destination nodes 3 and 11 are both available for EV #3 as shown in Fig. 11 (3), but for this EV, one of the charging positions is transportation node 18. The result is obtained from the global perspective, for the EVs that have limited charging demand. If charging location for EV # 3 is node 3, there is no EV can satisfy charging condition at node 18 due to long arrival distance, as shown in Equation (17), which may lead to less charging demand in the electrical energy network. Therefore, based on Equations (7) and (8), this condition violated the law of the worst charging.

In order to investigate the load margin of the distribution network and the capacity of holding EVs. Three cases are tested:

Case 1: growing annual rate of electricity load is 2.5%;
Case 2: growing annual rate of electricity load is 5%;
Case 3: growing annual rate of electricity load is 10%.

The simulation results are shown in Fig. 13 and Fig. 14, which depict the corresponding growing load margin and the largest number of EVs in areas respectively.

As it is clear to see from Fig. 13, the minimum power energy supplying margin occurs to this situation where the growing annual rate is 10%. The reason for this phenomenon is the limited capacity of power energy generation, on the other hand, the electricity load is increasing, which accounts large power energy consumption. The small value of the load margin indicates that the distribution network operating at high risk has a high probability of interrupting electrical energy.

Besides, from the view of the same level of growing electricity load, the growth margin has an evident decrease over time, which indicates the instability of electricity energy network continues to grow. In particular, for the growing annual rate of electricity load is 10%, the load margin below twice after 10 years. Thus, the results reflect that as the electricity load increases the electrical energy network becomes more and more unstable. Consequently, the charging load has to be reduced to ensure the security of the distribution network operation.

Fig. 14 represents the significant gap between each year and a vast difference in the number of EVs a give network can support in different electricity load level. For the worst level, the number of EVs is less than one third of the existing. This is unreasonable due to violations of the principle of the electrical energy network. The reason for such phenomenon as shown in Fig. 14 is that limiting available capacity of electrical energy determined by the existing structure of distribution network.

6. Conclusion

This paper provides a novel evaluation for impacts of mobile energy of EVs on distribution network coupling the interactions between vehicles energy network and electricity energy network in worse charging case. A model for generating the worst charging scenario is proposed, which includes the constraints of

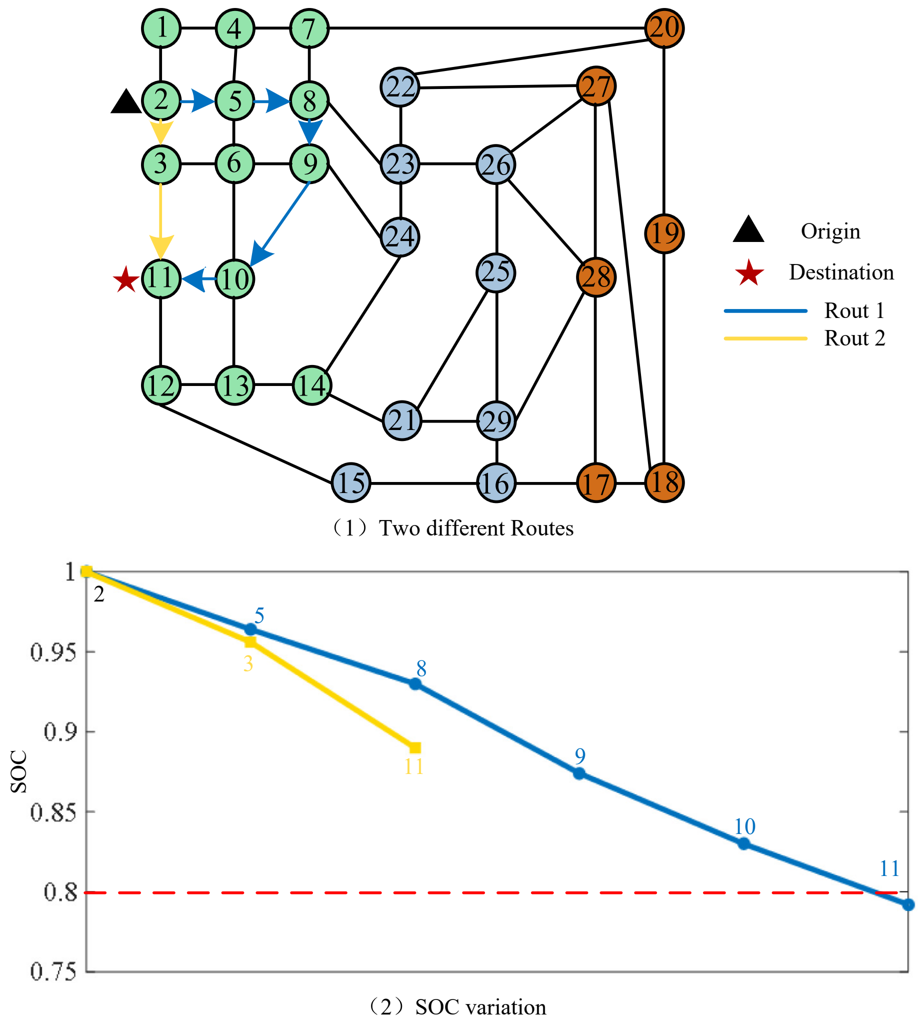

Fig. 12. Variation of SOC with different route.

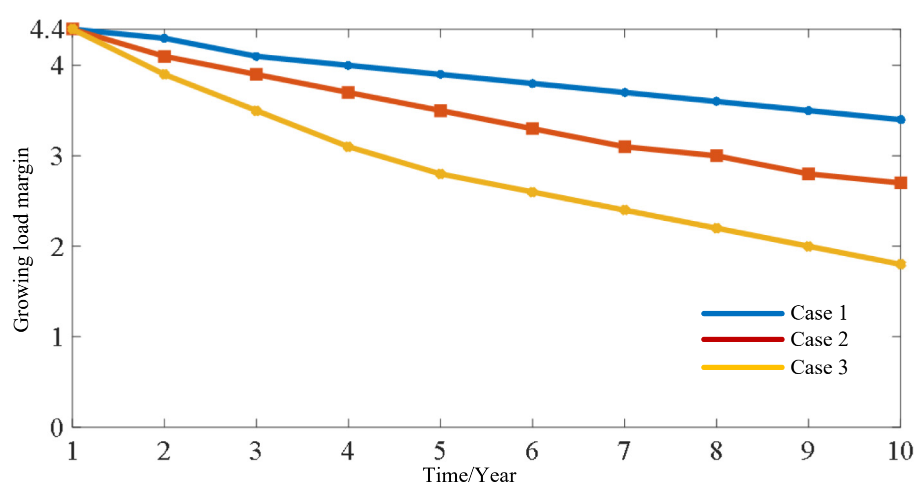

Fig. 13. Maximum margin in different growth rate of electricity load.

transportation network to EVs. Besides, in order to identify the limitation of the electrical network, an improved continue power flow calculation method considering EVs' integration is proposed, which is also used to calculate the allowed maximum number of EVs that a given network can supported. The evaluation results revealed that the weakest areas of a coupled energy network have a lot of common properties, and the impact of route choice and coupling relationship of the transportation and power grid on the

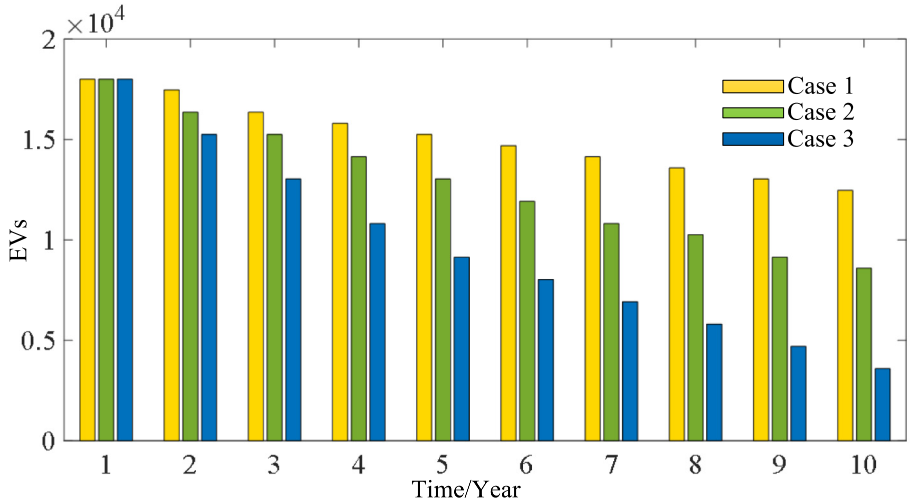

Fig. 14. Largest number of EVs in different growth rate of electricity load.

voltage margin limitation is emphasized.

In addition, this novel evaluation can be used to indicate the coupled network reformation and guide the EVs behavior to guarantee the voltage stability with a large amount of EVs integrated into the distribution network, which are also the future studies on this basis.

Declaration of competing interest

The authors declare that they have no known competing financial interests or personal relationships that could have appeared to influence the work reported in this paper.

Acknowledgement

This work was supported by Sichuan Science and Technology Program (2019YFH0171, 2019YFG0152, 20SYSX0233) and National Natural Science Foundation of China (51807127).

Nomenclature

$\boldsymbol{A}$	coupled network
$\boldsymbol{A}_{\mathrm{T}}$	transportation network
$\boldsymbol{A}_{\mathrm{P}}$	distribution network
$\boldsymbol{A}_{\mathrm{T\text{-}P}}$	coupling relationship between transportation network and distribution network
$a_{\mathrm{T},ab}$	information of transportation network node between a and b
$a_{\mathrm{T\text{-}P},aj}$	information between the transportation network node a and distribution network bus j
s_t	state of EV at time t
P_{c}	charging power
T_{c}	charging time
Q	battery capacity
ω	power consumption per mile
l	mileage
$\boldsymbol{V}$	set of nodes
$\boldsymbol{D}$	set of road length
n	number of transportation nodes
$v_{ab,0}$	the maximum accepted speed of road ab
$V_{ab}(t)$	traffic flow of road ab at time t
C_{ab}	road capacity of road ab
β_{ab}	saturation coefficient of road a
μ, γ, q	adaptive parameters of road
$\boldsymbol{L}_{ab}$	set of all feasible path between a and b
l_{ab}	the shortest path between a and b
F	objective function
F_{u}	deviation of actual voltage from the optimal value with the maximum margin
λ	penalty coefficient
$\boldsymbol{Y}$	optimal voltage of all buses
$\boldsymbol{H}(\boldsymbol{X})$	actual voltage of all buses
C_e	transmission power of line e
u_f	voltage of bus f
$C_e^{\max}$	upper limits for the transmission line e
$C_e^{\min}$	lower limits for the transmission line e
$u_f^{\max}$	upper and lower limits for the bus f
$u_f^{\min}$	lower limits for the bus f
N_{L}	set of transmission lines
M	number of buses
$\varepsilon(R)$	a function with 0 or 1
p	EV that satisfies the charging condition
N_{V}	number of EVs
s^p	state of EV p
P_{EV}	charging load
$\boldsymbol{G}_{\mathrm{P}}$	vectors of active power
$\boldsymbol{G}_{\mathrm{Q}}$	vectors of reactive power
$\boldsymbol{P}_0$	active power of electricity load
$\boldsymbol{Q}_0$	reactive power of electricity load
$\underline{\alpha}$	the minimum threshold coefficient of battery
α	threshold coefficient of charging condition
T_t	evaluation moment at time t
SOC_t^p	state of charging of EV p at time t
$P_{\mathrm{L},i}$	active power at bus i
$Q_{\mathrm{L},i}$	reactive power at bus i
$P_{\mathrm{L},i0}$	original active power at bus i
$Q_{\mathrm{L},i0}$	original reactive power at bus i
ζ_i	load parameter of bus i
$\boldsymbol{V}$	voltage amplitudes of all buses
$\boldsymbol{\Theta}$	voltage phases of all buses
$\boldsymbol{L}_{\mathrm{el}}$	set of electricity load
L_{k0}	original load of bus k
L_{k1}	the maximum load of bus k
$\delta_{k,\max}$	the maximum growth factor of bus k
θ_k	lower limit of bus k
δ_k	growth factor of bus k

Y_k	an increasing function from 0 to 1
$\boldsymbol{X}_k$	sampling electricity load
D_0	initial position of each EV
T_{start}	initial travel moment of each EV
$L_{k\_collapse}$	critical load at bus k
$\delta_{collapse}$	criterion of the voltage limit
$\boldsymbol{S}_{M\times N}$	integrated load growth factor
$\boldsymbol{S}_{M\times N^*}$	selected integrated load growth factor
$\boldsymbol{S}_{all}$	further selected integrated load growth factor
N_{sample}	sampling times
N	evaluating times

References

[1] Habib S, Khan MM, et al. A comprehensive study of implemented international standards, technical challenges, impact and prospects for electric vehicles. IEEE Access 2018;6:13866–90.
[2] Hu X, S. J. Moura, et al. "Integrated optimization of battery sizing, charging, and power management in plug-in hybrid electric vehicles," IEEE Trans Contr Syst Technol, vol. 24, no. 3, pp: 1036-1043.
[3] Hu X, Zou Y, Yang Y. Greener plug-in hybrid electric vehicles incorporating renewable energy and rapid system optimization". Energy 2016;111:971–80.
[4] Wu X, Hu X, et al. Stochastic control of smart energy management with plug-in electric vehicle battery energy storage and photovoltaic array. J. Power Sour 2016;333:203–12.
[5] Zhou L, Li F, et al. Cost/benefit assessment of a smart distribution system with intelligent electric vehicle charging. IEEE Trans Smart Grid 2014;5(2):839–47.
[6] Dickerman L, Harrison J. A new car, a new grid. IEEE Power Energy Mag 2010;8(2):55–61.
[7] Kadurek P, Ioakimidis CS, et al. Electric vehicles and their impact to the electric grid in S. Miguel. In: Proceedings of international Conference on power engineering. Lisbon, Portugal: Energy and Electrical Drives; 2009. p. 49–54.
[8] Shariff N, Essa M, Cipcigan L. Probabilistic analysis of electric vehicles charging load impact on residential distribution networks. In: IEEE international energy conference, Leuven, Belgium; 2016. p. 251–7.
[9] Zheng Y, Sun J, et al. Study of voltage stability margin for the distribution network with electric vehicle integration. Trans China Electrotech Soc 2014;29(8):20–6.
[10] Du X, Liu Y, et al. Modeling of random load of electric vehicle and its influence on node voltage distribution of distribution network. Electric Power Automation Equipment 2018;38(6). 124-120.
[11] Zheng J, Dai M, et al. Load cluster characteristic and modeling of EV charge station in residenttial district. Proceedings of the CSEE 2012;32(22):32–8.
[12] Xu W, Lv L, et al. Calculation of charging demand from electric vehicles based on Markov chain. Proc CSU-EPSA 2017;29(33):12–9.
[13] Wang Z, Fan S, et al. Coordinated charging strategy of plug-in electric vehicles for maximizing the distributed energy based on time and location. J Eng 2017;13:1740–4. 2017.
[14] Zhu X, Han H, et al. A multi-stage optimization approach for active distribution network scheduling considering coordinated electrical vehicle charging strategy. IEEE Access 2018;6:50117–30.
[15] Thomas D, D'Hoop G, et al. An integrated tool for optimal energy scheduling and power quality improvement of a microgrid under multiple demand response schemes. Appl Energy 2020;260:114314.
[16] Sun B, Huang Z, Tan X, et al. Optimal scheduling for electric vehicle charging with discrete charging levels in distribution grid. IEEE Transactions on Smart Grid 2018;9(2):624–34.
[17] Cheng Y, Zhang C. Configuration and operation combined optimization for EV battery swapping station considering PV consumption bundling. Protection and Control of Modern Power Systems 2017;2(2):276–93.
[18] Bayati M, Abedi M, et al. Short-term interaction between electric vehicles and micgrid in decentralized vehicle-to-grid control methods. Protection and Control of Modern Power Systems 2019;4(4):42–52.
[19] Cai H, Chen Q, et al. Day-ahead optimal charging/discharging scheduling for electric vehicles in micogrids. Protection and Control of Modern Power Systems 2018;3(3):93–107.
[20] Chen L, Vincentelli AS, et al. Driving-style-based codesign optimization of an automated electric vehicle: a cyber-physical system approach. IEEE Trans Ind Electron 2019;66(4):2965–75.
[21] Hu X, Wang H, et al. Cyber-physical control for energy-saving vehicle following with connectivity. IEEE Trans Ind Electron 2017;64(11):8578–87.
[22] Jiang R, Zhang Z, et al. A coordinated charging strategy for electric vehicles based on multi-objective optimization. In: *2nd International conference on power and renewable energy*, Chengdu, China; 2017. p. 823–7.
[23] Chen H, Hu Z, et al. Coordinated charging strategies for electric bus fast charging stations. In: IEEE PES Asia-pacific power and energy conference, Xi'an, China; 2016. p. 1174–9.
[24] Zheng L, Hu W, et al. A novel method to monitor and predict voltage collapse: the critical transitions approach. IEEE Trans Power Syst 2018;33(2):1184–94.
[25] Mohamed AA, Venkatesh B. Line-wise power flow and voltage collapse. IEEE Trans Power Syst 2018;33(4):3768–78.
[26] Kamel M, Karrar AA, et al. Development and application of a new voltage stability index for on-line monitoring and shedding. IEEE Trans Power Syst 2018;33(2):1231–41.
[27] Zhang H, Moura S, et al. PEV fast-charging station siting and sizing on coupled transportation and power networks. IEEE Trans. Smart Grid 2018;9(4): 2595–604.
[28] Alizadeh M, Wai H, et al. Optimal pricing to manage electric vehicles in coupled power and transportation networks. IEEE Tans. Control Net. Syst. 2017;4(4):863–75.
[29] Hou K, Xu X, et al. A reliability assessment approach for integrated transportation and electrical power systems incorporating electric vehicles. IEEE Trans. Smart Grid 2018;9(1):88–100.
[30] Tian L, Shi S, et al. A statistical model for charging power demand of electric vehicles. Power Syst Technol 2010;34(11):126–30.
[31] Chen L, Nie Y, Zhong Q. A model for electric vehicle charging load forecasting based on trip chains. Trans China Electrotech Soc 2015;30(4):216–25.
[32] Yan Z, Zhang R, et al. Price and period research of electric vehicles charging and discharging based on demand response. Power System Protection and Control 2018;46(15):16–22.
[33] Chen T, Zhang B, et al. Optimal routing and charging of an electric vehicle fleet for high-efficiency dynamic transit systems. IEEE Transactions on Smart Grid 2018;9(4):3563–72.
[34] Chen S. Research on practical velocity-volume model of urban street. Southeast University; 2004.
[35] Liu R, Chen J, Chen S. Improvement of Warshall algorithm based on transitive closure. Comput Eng 2015;31(19):38–9.
[36] Xu D, Cai M, Chen Y. Shortest path of urban traffic based on the improved Floyd algorithm. Electronic Sci & Tech. 2017;30(7):17–20.
[37] Burchett S, Douglas D, et al. An optimal thevenin equivalent estimation method and its application to the voltage stability analysis of a wind hub. IEEE Trans Power Syst 2018;33(4):3644–52.
[38] Chiang HD, Flueck AJ. A practical tool for tracing power system steady-state stationary behavior due to load and generation variations. IEEE Trans Power Syst 1995;10(2):623–34.
[39] Li SH, Chiang HD. Nonlinear predictors and hybrid corrector for fast continuation power flow. IET Gener, Transm Distrib 2008;2(3):341–54.
[40] Yu H, Zhong Z, et al. A probabilistic load flow calculation method with Latin hypercube sampling. Autom Electr Power Syst 2009;33(21):32–5.
[41] Owen AB. Controlling correlations in Latin hypercube samples. J Am Stat Assoc 1994;89(428):1517–22.
[42] Shao Y, Mu Y, et al. A spatial-temporal charging load forecast and impact analysis method for distribution network using EVs-Traffic-Distribution model. Proceedings of the CSEE 2017;37(18):5207–19.
[43] Xiang Y, Liu J, et al. Economic planning of electric vehicle charging stations considering traffic constraints and load profile templates. Appl Energy 2016;178(15).
[44] Axsen J, Burke A, Kurani K. Batteries for plug-in hybrid electric vehicles (PHEVs): goals and the state of technology circa. Inst. Transportation Studies, Univ. California; 2008.